II CONGRESSO NACIONAL DE ENGENHARIA MECÂNICA
II NATIONAL CONGRESS OF MECHANICAL ENGINEERING
12 a 16 de Agosto de 2002 - João Pessoa – PB

APPLICATION OF THE MULTIGRID CORRECTION-STORAGE FORMULATION TO THE SOLUTION OF INCOMPRESSIBLE LAMINAR FLOW

José Antonio Rabi
Departamento de Energia – IEME, Instituto Tecnológico de Aeronáutica – ITA
12.228-900 - São José dos Campos - Brazil

Marcelo J.S. De-Lemos
Departamento de Energia – IEME, Instituto Tecnológico de Aeronáutica – ITA
12.228-900 - São José dos Campos - Brazil, delemos@mec.ita.br

Abstract. *Multigrid methods are known to reduce computational time of iterative solutions and have been extensively used in CFD problems. In this paper, a correction storage multigrid formulation following a V-cycle strategy is implemented to numerically solve steady-state 2-dimensional incompressible laminar recirculating flows. Structured, orthogonal and irregular meshes are used to perform finite volume discretization. Pressure-velocity coupling is accomplished through the SIMPLE method while the TDMA algorithm relaxes the resulting algebraic equation system. The solution method is numerically validated against the results from a laminar flow between parallel plates whereas recirculating flow patterns are graphically presented. Advantages of employing more than one grid level and of using the CS approach are discussed upon.*

Key words: *multigrid method, laminar flow, numerical simulation, finite volume*

1. INTRODUCTION

Computational Fluid Dynamics (CFD) has experienced improvements related not only to the availability of fast and high memory capacity computers but also to the application of efficient iterative methods. Numerical simulation is already incorporated into the solution of engineering problems like energy generation processes, environmental phenomena and flight engineering. In these problems, fluid flow is present and should be properly described.

Design and optimization often require accurate results. However, well-refined meshes tend to increase the computational effort. Multigrid methods achieve convergence acceleration by iterating at a sequence of gradually less refined grids instead of iterating at a single grid.

Depending on how variables are handled in coarse meshes, i.e., in all meshes but the finest, multigrid algorithms may be implemented following two distinct formulations: correction storage (CS) and full approximation storage (FAS). In the first formulation, algebraic equations in coarse meshes are solved for the corrections of the unknowns. In the other formulation, the unknowns themselves are operated in all grid levels.

Previous works (Hackbusch, 1985; Stüben and Trottenberg, 1982; Brandt, 1977) recommend the application of the CS formulation when solving linear problems whereas the FAS formulation is more suited for non-linear situations. Nevertheless, Jiang et al. (1991) reported the numerical solution of the Navier-Stokes (non-linear) equations using the multigrid CS formulation.

Motivated by this prior instance, this work applied a multigrid CS-formulation method to solve steady-state 2-dimensional incompressible laminar recirculating flows. Actually, it resulted from a

preliminary attempt to incorporate a multigrid algorithm to an existing single-grid computational program to solve flow problems. The numerical method also included finite volume discretization, the SIMPLE pressure-velocity coupling and TDMA iterative relaxation (Patankar, 1980; Patankar and Spalding, 1972).

2. MATHEMATICAL MODEL

In this work, no heat transfer is considered. Hence, the fluid flow is governed by the continuity and the Navier-Stokes equations. Assuming steady state condition, these set of equations in a 2-dimension Cartesian coordinate frame are written as (Bird at al., 1960)

$$\frac{\partial}{\partial x}(\rho U)+\frac{\partial}{\partial y}(\rho V)=0 \tag{1}$$

$$\frac{\partial}{\partial x}(\rho U^2)+\frac{\partial}{\partial y}(\rho VU)=\frac{\partial}{\partial x}\left(\mu\frac{\partial U}{\partial x}\right)+\frac{\partial}{\partial y}\left(\mu\frac{\partial U}{\partial y}\right)-\frac{\partial P}{\partial x}+s_{\mathrm{U}} \tag{2}$$

$$\frac{\partial}{\partial x}(\rho UV)+\frac{\partial}{\partial y}(\rho V^2)=\frac{\partial}{\partial x}\left(\mu\frac{\partial V}{\partial x}\right)+\frac{\partial}{\partial y}\left(\mu\frac{\partial V}{\partial y}\right)-\frac{\partial P}{\partial y}+s_{\mathrm{V}} \tag{3}$$

where U and V are the velocity vector components and P is the pressure. The fluid density ρ and viscosity μ are assumed to be constant, so that the continuity equation, Eq. (1), can be handled to show that the viscous source terms s_{U} and s_{V} are both null. Since the resulting momentum equations contain similar terms, they can be expressed under a general form, namely,

$$\frac{\partial}{\partial x}(\rho U\phi)+\frac{\partial}{\partial y}(\rho V\phi)=\frac{\partial}{\partial x}\left(\Gamma_\phi\frac{\partial\phi}{\partial x}\right)+\frac{\partial}{\partial y}\left(\Gamma_\phi\frac{\partial\phi}{\partial y}\right)+S_\phi \tag{4}$$

where $\phi = U, V$ represents the flow variable to be numerically solved, $\Gamma_\phi = \mu$ is the corresponding diffusive coefficient and S_ϕ contains the pressure gradient, in this case.

3. NUMERICAL METHOD DESCRIPTION

3.1. Finite Volume Discretization

Each solution domain was divided into rectangular different-sized control volumes (CVs), assembling a structured orthogonal non-uniform mesh. Grid points were located according to a cell-centered scheme and variables were stored in a collocated arrangement (Patankar, 1980). A typical CV is sketched in Fig. (1). Discretization was accomplished by double integrating Eq. (4) over the CV and this process has been presented elsewhere (Rabi and de Lemos, 2001; Rabi, 1998).

The flux blended deferred correction scheme (DCS) was used for nodal interpolation (Khosla and Rubin, 1974). In this scheme, interface values are approximated as a linear combination of central differencing scheme (CDS) and upwind differencing scheme (UDS) values according to

$$\phi_{\mathrm{face}}^{\mathrm{DCS}}=\lambda\phi_{\mathrm{face}}^{\mathrm{CDS}}+(1-\lambda)\phi_{\mathrm{face}}^{\mathrm{UDS}}=\phi_{\mathrm{face}}^{\mathrm{UDS}}+\lambda\left(\phi_{\mathrm{face}}^{\mathrm{CDS}}-\phi_{\mathrm{face}}^{\mathrm{UDS}}\right)^{*} \tag{5}$$

where the starred (*) quantities in the last parenthesis are numerical values from the previous iteration. The combination factor λ may vary from 0 (pure UDS) to 1 (pure CDS).

Substitution of all approximate expressions into the general momentum transport equation, Eq. (4), gives the following algebraic equation for a given grid node P

$$a_P \phi_P = a_E \phi_E + a_W \phi_W + a_N \phi_N + a_S \phi_S + b_\phi \quad (6)$$

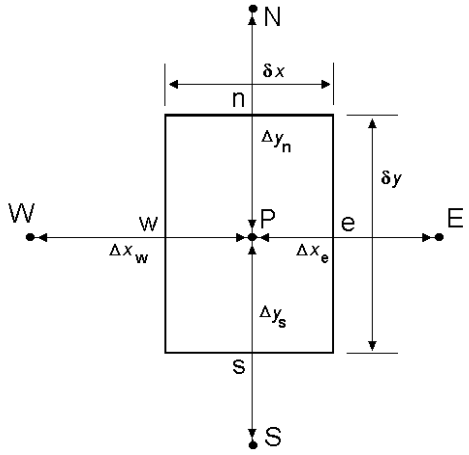

Figure 1. Sketch of a typical control volume (CV) to perform discretization.

For an example, the east interface coefficient a_E is of the form

$$a_E = \max[-C_e^*, 0] + \frac{\mu_e^* \delta y}{\Delta x_e} \quad (7)$$

The operator $\max[p,q]$ returns the greater of p and q. The remaining coefficients are defined similarly and they can be found in (Rabi, 1998).

The discretized source term b_ϕ contains contributions from the pressure gradient and from the DCS previous iteration values according to

$$b_\phi = S_\phi \delta v + \lambda \left(\sum_{nb} a_{nb}^{DCS} \phi_{nb}^* - a_P^{DCS} \phi_P^* \right) \quad (8)$$

Here $S_U \, \delta v = -(P_e - P_w)\delta y$ and $S_V \, \delta v = -(P_n - P_s)\delta x$. The subscript nb indicates that the summation is over all neighboring CVs to the CV containing point P.

3.2. Pressure-Velocity Coupling and Under-relaxation

Pressure-velocity coupling follows the SIMPLE – Semi-Implicit Method for Pressure-Linked Equations algorithm (Patankar and Spalding, 1972). The basic idea is to solve a pressure correction P' equation derived from the momentum and continuity equations, which is also of the form

$$a_P P_P' = a_W P_P' + a_E P_P' + a_S P_P' + a_N P_P' - S_m \quad (9)$$

Definitions for all coefficients a_i and for the mass imbalance source term S_m are found in (Patankar and Spalding, 1972).

The resulting set of equations is non-linear and coupled. Moreover, some terms are neglected when the pressure correction equation, Eq. (9), is obtained. Accordingly, the SIMPLE algorithm tends to diverge if no under-relaxation is employed. Therefore, the pressure correction is given by

$$P_P = P_P^* + \xi_{P'} P_P' \quad (10)$$

while the velocity components are under-relaxed according to

$$\frac{a_P}{\xi_U}U_P = \sum_{nb} a_{nb}U_{nb} + b_U + (1-\xi_U)\frac{a_P}{\xi_U}U_P^* \quad \text{and} \quad \frac{a_P}{\xi_V}V_P = \sum_{nb} a_{nb}V_{nb} + b_V + (1-\xi_V)\frac{a_P}{\xi_V}V_P^* \qquad (11)$$

The relaxation factors $\xi_{P'}$, ξ_U and ξ_V need not be the same.

3.4. Multigrid Correction Storage Method

Convergence of the numerical solution is fast in the beginning of calculations, slowing down sensibly as the iterative process goes on. This is because the smoothing algorithm can efficiently reduce only those Fourier error components whose wavelengths are smaller than or comparable to the grid spacing (Hackbusch, 1985; Stüben and Trottenberg, 1982; Brandt, 1977). In other words, a given error wavelength can be properly smoothed only at a grid having an adequate mesh spacing.

The rationale of multigrid methods is to accelerate convergence by covering a broader error wavelength spectrum by iterating at a sequence of gradually less refined grids instead of iterating at a single grid. Long error wavelengths in a fine mesh become smaller in a coarse one, where they can be appropriately smoothed out. Hence, in each grid level visited by the solution process, the corresponding error components are efficiently reduced, which speeds up convergence.

Writing Eq. (6) for each CV in the solution domain results in an equation system of the form

$$\mathbf{A}_k \boldsymbol{\Phi}_k = \mathbf{b}_k \qquad (12)$$

where $\mathbf{A}_k$ is the matrix of coefficients, $\boldsymbol{\Phi}_k$ is the matrix of unknowns and $\mathbf{b}_k$ contains the source terms. Index k refers to a given grid level, being $k = 1$ for the coarsest and $k = M$ for the finest.

Motivated by Jiang et al. (1991), this work implements a multigrid CS method, although this formulation is not recommended to solve non-linear problems. On the other hand, restriction operations in the CS formulation are relatively simpler to implement than theirs FAS formulation counterparts. Coarse grid approximations are obtained for the correction of the flow unknown being numerically solved, i.e., $\boldsymbol{\Phi}_k$ stores the flow unknown itself only when $k = M$, whereas $\boldsymbol{\Phi}_k$ stores corrections for this unknown for all $k < M$.

Relaxing the equation system, Eq. (12), by a number of smoothing iterations, an intermediate value $\overline{\boldsymbol{\Phi}}_k$ is available along with its correction $\boldsymbol{\phi}_k = \boldsymbol{\Phi}_k - \overline{\boldsymbol{\Phi}}_k$. Defining the residue as

$$\mathbf{r}_k = \mathbf{b}_k - \mathbf{A}_k \overline{\boldsymbol{\Phi}}_k \qquad (13)$$

it is shown (Hackbusch, 1985; Stüben and Trottenberg, 1982; Brandt, 1977) that the correction $\boldsymbol{\phi}_k$ itself is the solution of another linear system

$$\mathbf{A}_k \boldsymbol{\phi}_k = \mathbf{r}_k \qquad (14)$$

which is of the same form of Eq. (12). In an adjacent coarser grid, Eq. (14) is approximated by

$$\mathbf{A}_{k-1} \boldsymbol{\phi}_{k-1} = \mathbf{r}_{k-1} \quad , \quad \mathbf{r}_{k-1} = I_k^{k-1}\mathbf{r}_k \qquad (15)$$

The restriction operator I_k^{k-1} transfers values from grid k to its adjacent coarser grid $k-1$.

After being relaxed, the coarse grid approximation $\overline{\boldsymbol{\phi}}_{k-1}$ for the correction is taken back to the adjacent fine grid through the prolongation operator I_{k-1}^k

$$\overline{\boldsymbol{\phi}}_k = I_{k-1}^k \overline{\boldsymbol{\phi}}_{k-1} \qquad (16)$$

in order to refine the intermediate value $\overline{\mathbf{\Phi}}_k$ according to

$$\mathbf{\Phi}_k^{new} = \overline{\mathbf{\Phi}}_k + \overline{\boldsymbol{\phi}}_k \tag{17}$$

All these numerical operations, Eqs. (12)–(17), are concatenated through all available k values (i.e. grid levels). The sequence as how the iteration process migrates from one grid level to another is what distinguishes the so-called V-cycle from the W-cycle (Hackbusch, 1985). In the present paper, only V-cycling strategies are considered.

The residue restriction in Eq. (15) is accomplished by summing up the residues corresponding to the equations of the four fine grid CVs that compose the coarse grid one, as sketched in Fig. (2). Indexes ij and IJ locate the CV in the fine grid and in the coarse grid respectively.

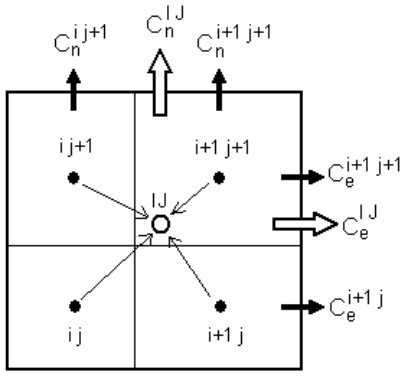

Figure 2. Restriction procedures: mass flux and residue summation.

Convective and diffusive terms of matrix $\mathbf{A}_k$, Eq. (7), also undergo restriction. Diffusive terms are recalculated after each grid level change since they depend on the grid geometry. Fine grid convective fluxes are summed up at control volume faces in order to compose the corresponding coarse grid flux, as shown in Fig. (2) (west and south face fluxes are not pictured for clarity). Such restriction procedures are commonly used in the literature (Bai et al., 1994; Sathyamurthy and Patankar, 1994; Jiang et al., 1991; Joshi and Vanka, 1991; Hortmann et al., 1990; Peric et al., 1989; Hutchinson at al., 1988; Hutchinson and Raithby, 1986).

The prolongation operator I_{k-1}^{k} is numerically accomplished via bilinear interpolation (Bai et al., 1994; Jiang et al., 1991; Joshi and Vanka, 1991; Hortmann et al., 1990; Peric et al., 1989; Thompson and Ferziger, 1989; Vanka, 1986). In this work, such operator is implemented over a non-uniform grid. The idea is to use an intermediate mesh between adjacent fine and coarse grids to store values $\phi_{aux}^{I\,j}$ resulting from the application of the operator along one coordinate (say y) in the coarse grid. Then, the operator is again applied along the remaining coordinate (x) in order to obtain the fine grid values, as sketched in Fig. (3). Linear interpolation is evoked in both directions.

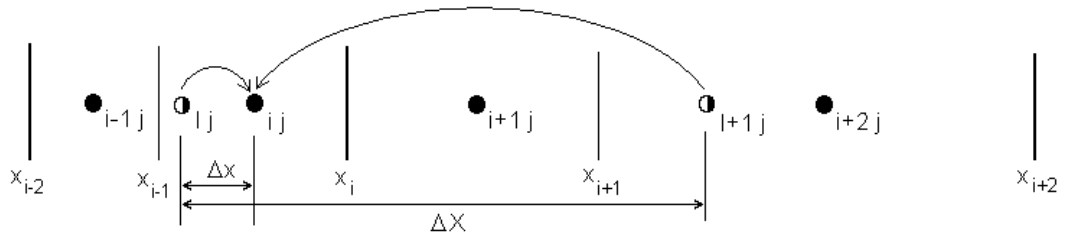

Figure 3. Prolongation: recovering the fine grid from the auxiliary grid.

4. RESULTS

Flow geometries and boundary conditions studied in this work are sketched in Figs. (4*a*–*d*). Although there is no recirculation in the flow corresponding to Fig. (4*a*), its developed velocity profile can be analytically described and hence it is useful to validate the numerical method.

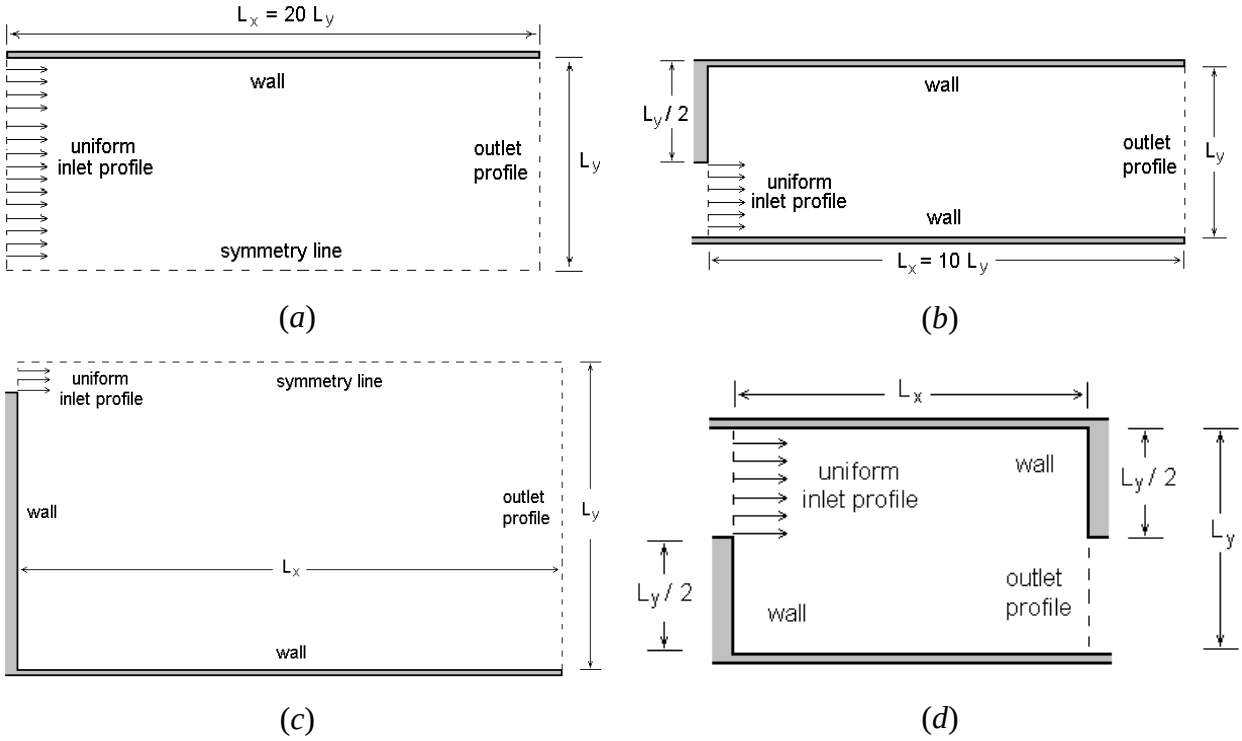

Figure 4. Laminar flow geometries and boundary conditions considered in this paper: (*a*) parallel plates; (*b*) backward facing step; (*c*) confined jet; (*d*) rectangular tank.

Accordingly, the solution method was initially tested against the laminar flow between parallel plates, Fig. (4*a*). In the outlet region where the flow is fully developed, the *U*-velocity component profile is analytically expressed by (Shah and London, 1978)

$$U(y) = \frac{3}{2} U_{\mathrm{O}} \left[1 - \left(\frac{y}{L_{\mathrm{y}}} \right)^2 \right] \tag{18}$$

Adopted values were $L_{\mathrm{y}} = 0.05$ m , $L_{\mathrm{x}} = 1.0$ m , $U_0 = 0.1$ m/s , $\rho = 1.0$ kg/m^3 , $\mu = 10^{-4}$ kg/m.s , $\xi_{\mathrm{U}} = 0.8$, $\xi_{\mathrm{V}} = 0.6$ and $\xi_{\mathrm{P'}} = 0.05$. The V-cycling strategy was fixed at 1 pre-smoothing and 1 post-smoothing iteration ($\nu^{\mathrm{pre}} = \nu^{\mathrm{post}} = 1$) and 5 coarsest grid iterations ($\nu^{\mathrm{cg}} = 5$). Pure UDS ($\lambda = 0$) was employed as interpolation scheme and there were 160 CVs along the x direction (*NI*) and 32 CVs along the y direction (*NJ*). A good agreement between the 4-grid numerical solution and the exact solution, Eq. (18), can be verified, as shown by Fig. (5).

The normalized residues reduction histories for the velocity components and for the pressure correction of the 4-grid (indicated as 4g) and the 1-grid (1g) solution of this laminar flow are pictured in Fig. (6). Residues are calculated and normalized in the finest grid level according to

$$R_{\phi} = \sqrt{\frac{\sum_{\mathrm{ij}} \left(r_{\mathrm{M}}^{\mathrm{ij}} \right)^2}{(NI-2)(NJ-2)}} \quad , \quad \text{where} \quad r_{\mathrm{M}}^{\mathrm{ij}} = a_{\mathrm{P}} \phi_{\mathrm{P}} - \left(\sum_{\mathrm{nb}} a_{\mathrm{nb}} \phi_{\mathrm{nb}} \right) \quad (\phi = U, V) \tag{19}$$

In terms of CPU time spent to run the program until convergence, it is observed that the 4-grid algorithm has better performance than the 1-grid algorithm.

The influence of the grid refining (i.e. grid size) on the multigrid algorithm performance, using a given number M of grid levels, is verified in Tab. (1). The ratio of the 1-grid computing time to the M-grid time is presented in the last column. Such time ratio can be thought of as a measure of the relative computational effort saving. It is worth noting that savings increase as grids become finer and such feature is what makes multigrid methods interesting.

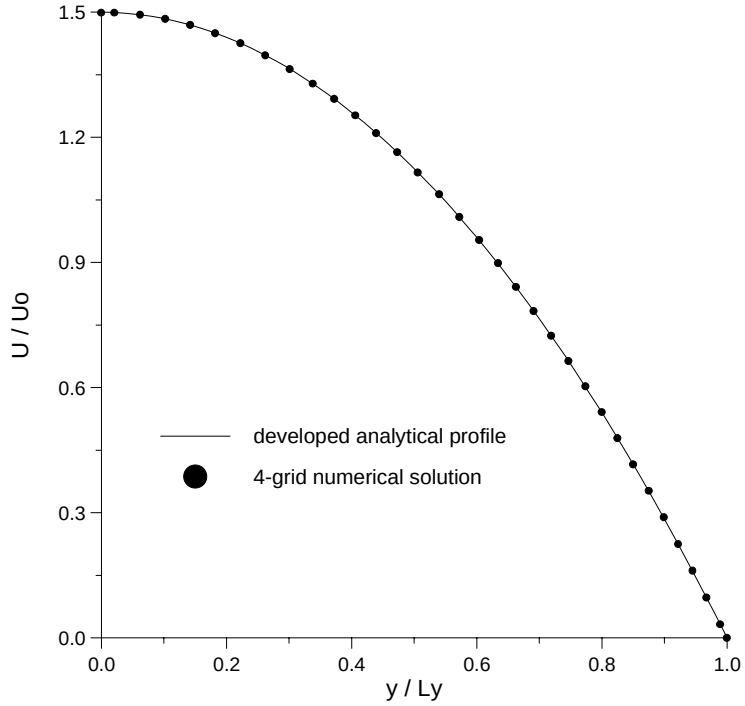

Figure 5. Laminar flow between parallel plates: numerical validation of 4-grid solution.

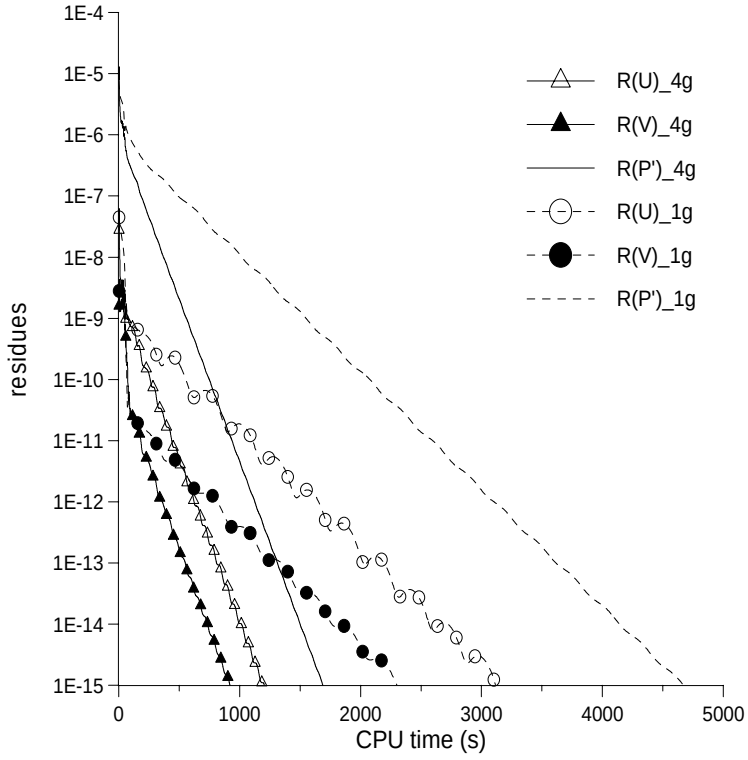

Figure 6. Flow between parallel plates: U, V and P' residue reduction histories.

Table 1. Flow between parallel plates: grid-refining influence on the computational effort.

NI x *NJ*	*M*	R_U (x 10^{-18})	R_V (x 10^{-20})	$R_{P'}$ (x 10^{-16})	t_M (s)	t_1 / t_M
160 x 32	4	2.76	9.22	9.95	1688.4	2.768
	3	2.01	6.59	10.0	1874.3	2.493
	2	1.29	4.74	9.99	1912.1	2.444
	1	1.70	3.56	9.87	4672.8	1
240 x 32	4	3.53	21.0	9.99	2615.4	4.066
	3	2.71	11.6	9.93	3218.2	3.304
	2	1.67	8.11	10.0	3457.1	3.076
	1	2.34	5.85	10.0	10634.5	1
320 x 32	4	6.56	53.0	9.98	2919.0	4.474
	3	3.07	17.5	9.95	3251.6	4.017
	2	3.44	13.0	9.93	3626.1	3.602
	1	3.85	12.7	9.95	13060.8	1

Recirculating flows, Figs. (4*b–d*), are considered next. Table (2) summarizes all geometric and physical values concerning the cases studied. Pure UDS ($\lambda = 0$) was again employed. Figures (7*a–c*) help to qualitatively visualize the flow field patterns obtained from multigrid numerical solutions. The recirculating regions can be clearly seen.

Table 2. Summary of values adopted for the recirculating flows.

Flow type	Backward facing step	Confined jet	Rectangular tank
L_x (m)	0.5	2.0	0.8
L_y (m)	0.05	0.5	0.6
U_0 (m/s)	0.2	0.01	0.01
ρ (kg/m^3)	1.0	1.0	1.0
μ (kg/m.s)	10^{-4}	10^{-4}	10^{-4}
NI x *NJ*	144 x 48	160 x 64	128 x 96
ξ_U , ξ_V , $\xi_{P'}$	0.8 , 0.6 , 0.03	0.8 , 0.6 , 0.01	0.8 , 0.6 , 0.01
ν^{pre}, ν^{post}, ν^{cg}	1 , 1 , 5	1 , 1 , 1	1 , 1 , 1

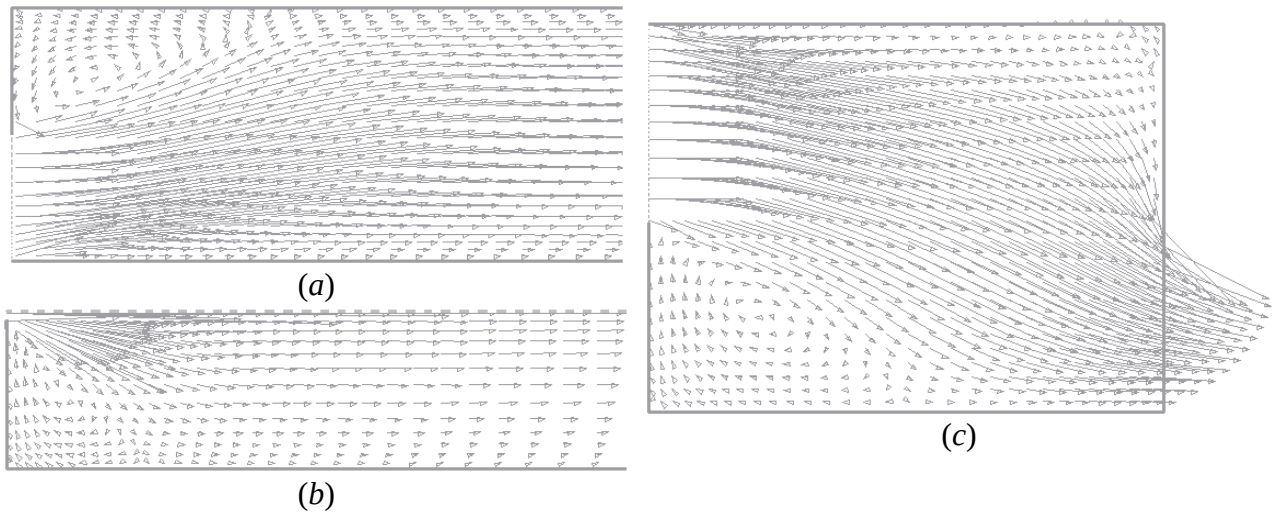

(*a*)

(*b*)

(*c*)

Figure 7. Flow field visualization (obtained from multigrid solutions):
(*a*) backward facing step; (*b*) confined jet; (*c*) rectangular tank.

Residue levels and computational efforts (in terms of CPU time spent) from solutions using different numbers M of grid levels are displayed and compared in Tab. (3). The last column shows the ratio of the single-grid solution time (t_1) to the multigrid one (t_M). Again, this ratio can be seen as a measure of the relative computational effort economy. It is seen that in general this economy increases as the number of grids used enlarges.

Table 3. Recirculating flows: computational effort results.

Flow type	M	R_U (x 10^{-18})	R_V (x 10^{-19})	$R_{P'}$ (x 10^{-16})	t_M (s)	t_1 / t_M
Backward facing step	4	2.99	3.96	9.92	1608.3	2.962
	3	2.54	3.62	9.91	1797.0	2.562
	2	2.52	4.78	9.95	1765.0	2.608
	1	1.43	1.71	9.96	4603.0	1
Confined jet	3	0.194	0.389	9.13	1558.6	4.833
	2	0.997	1.37	9.60	3756.6	2.005
	1	1.85	2.20	9.05	7533.1	1
Rectangular tank	3	3.27	2.12	9.96	3887.8	2.098
	2	2.55	2.07	9.96	4703.8	1.733
	1	2.60	1.62	9.92	8158.0	1

However, there may be a limiting number of grid levels to be employed. For instance, the confined jet multigrid solution employs 3 grid levels at most because only 4 finest grid CVs are used to perform the inlet region and using a fourth grid level would make the left upper corner CV to be requested by 2 distinct boundary conditions (namely, inlet flow and wall). Divergence was observed when a fourth grid level was used to solve the flow through rectangular tank problem. This may suggest that the corresponding coarsest grid (16 x 12) was not fine enough to handle properly the recirculating regions.

Results show that the application of the multigrid technique can speed up the iterative algorithm by values varying from 1.7 up to 4.8 times (in terms of CPU time), depending on the flow geometry and the number of grids employed. Considering multigrid standards, these poor results suggest that a multigrid FAS formulation may be more adequate for circulating flow problems. As far as flow pattern is concerned, the convergence rate acceleration did not jeopardize qualitatively the expected results as pictured in Fig. (7).

3. CONCLUSIONS

A multigrid technique was applied to solve 2-dimension laminar recirculating flow problems. The numerical method included finite volume discretization and SIMPLE pressure-velocity coupling. Structured, orthogonal and non-uniform meshes were used and the algebraic equation system was relaxed by the TDMA algorithm. Multigrid was implemented following a correction storage formulation and only V-cycle strategy was considered. Solution method was numerically validated by an existing analytical profile. All results showed slightly better performance of multigrid solutions when compared to their 1-grid counterpart, without jeopardizing qualitatively the flow field pattern. Convergence accelerations up to 4.8 times were observed, which suggest that a full approximation storage formulation may actually be more adequate.

4. ACKNOWLEDGMENT

The authors would like to thank CNPq for their financial support throughout this research, undertaken at the Laboratório de Computação em Fenômenos de Transporte LCFT/ITA, São José dos Campos, SP.

5. REFERENCES

Bai, L., Mitra, N.K., Fiebig, M.C. and Kost, A., 1994, "A multigrid method for predicting periodically fully developed flow", Int. J. Num. Meth. Fluids, Vol. 18, pp. 843-852.

Bird, R.B., Stewart, W.E. and Lightfoot, E.N., 1960, "Transport Phenomena", John Wiley & Sons, New York.

Brandt, A., 1977, "Multi-level adaptive solutions to boundary-value problems", Math. Comp., Vol. 31, No. 138, pp. 333-390.

Stüben, K. and Trottenberg, U., 1982, "Multigrid Methods", IN: Lect. Notes Math., Springer-Verlag, Berlin, Vol. 960, pp. 1-76.

Hackbusch, W., 1985, "Multi-Grid Methods and Applications", Springer-Verlag, Berlin.

Hortmann, M., Peric, M. and Scheuerer, G., 1990, "Finite volume multigrid prediction of laminar convection: benchmark solutions", Int. J. Num. Meth. Fluids, Vol. 11, pp. 189-207.

Hutchinson, B.R., Galpin, P.F. and Raithby, G.D., 1988, "Application of Additive Correction Multigrid to the Coupled Fluid Flow Equations", Numerical Heat Transfer, Vol. 13, No. 2, pp. 133-147.

Hutchinson, B.R. and Raithby, G.D., 1986, "A Multigrid Method Based on the Additive Correction Strategy", Numerical Heat Transfer, Vol. 9, No. 5, pp. 511-537.

Jiang, Y., Chen, C.P. and Tucker, P.K., 1991, "Multigrid solutions of unsteady Navier-Stokes equations using a pressure method", Num. Heat Transfer – part A, Vol. 20, pp. 81-93.

Joshi, D.S. and Vanka, S.P., 1991, "Multigrid calculation procedure for internal flows in complex geometries", Num. Heat Transfer – Part B, Vol. 20, pp. 61-80.

Khosla, P.K. and Rubin, S.G., 1974, "A diagonally dominant second-order accurate implicit scheme", Comput. Fluids, Vol. 2, No. 12, pp. 207.

Patankar, S.V., 1980, "Numerical Heat Transfer and Fluid Flow", Hemisphere Publishing Corporation, New York.

Patankar, S.V. and Spalding, D.B., 1972, "A calculation procedure for heat, mass and momentum transfer in three-dimensional parabolic flows", Int. J. Heat Mass Transfer, Vol. 15, pp. 1787-1806.

Peric, M., Rüger, M. and Scheuerer, G., 1989, "A finite volume multigrid method for calculating turbulent flows", IN: Seventh Symposium on Turbulent Shear Flows, pp. 7.3.1-7.3.6, Stanford University.

Rabi, J.A., 1998, "Aplicação do método multigrid na solução numérica de problemas 2-D simples de mecânica dos fluidos e transferência de calor", Dissertação de Mestrado, Depto. Energia, Divisão de Engenharia Mecânica-Aeronáutica, Instituto Tecnológico de Aeronáutica, São José dos Campos.

Rabi, J.A. and de Lemos, M.J.S., 2001, "Optimization of convergence acceleration in multigrid numerical solutions of conductive-convective problems", Applied Math. Comp., Vol. 124, N. 2, pp. 215-226.

Sathyamurthy, P.S. and Patankar, S.V., 1994, "Block-Correction-Based Multigrid Method for Fluid Flow Problems", Numerical Heat Transfer – Part B, Vol. 25, pp. 375-394.

Shah, R. K. and London, A. L., 1978, "Laminar flow forced convection in ducts", IN: Advances in Heat Transfer, Academic Press, New York.

Thompson, M.C. and Ferziger, J.H., 1989, "An adaptive multigrid technique for the incompressible Navier-Stokes equations", J. Comp. Phys., Vol. 82, pp. 94-121.

Vanka, S.P., 1986, "Block-implicit multigrid calculation of two-dimensional recirculating flows", Comp. Meth. Appl. Mech. Eng., Vol. 86, pp. 29-48.